J. Astrophys. Astr. (2012) **33,** 375–386

On the Maximum Separation of Visual Binaries

M. I. Nouh[1,*] & M. A. Sharaf[2]

[1]*Department of Physics, College of Science, Northern Border University, 1321 Arar, Saudi Arabia*

[2]*Department of Astronomy, Faculty of Science, King Abdul-Aziz University, Jeddah, Saudi Arabia*

[*]*e-mail: abdo_nouh@hotmail.com*

Received 2012 May 5; accepted 2012 May 30

Abstract. In this paper, an efficient algorithm is established for computing the maximum (minimum) angular separation $\rho_{\max}(\rho_{\min})$, the corresponding apparent position angles $(\theta|_{\rho_{\max}}, \theta|_{\rho_{\min}})$ and the individual masses of visual binary systems. The algorithm uses Reed's formulae (1984) for the masses, and a technique of one-dimensional unconstrained minimization, together with the solution of Kepler's equation for $(\rho_{\max}, \theta|_{\rho_{\max}})$ and $(\rho_{\min}, \theta|_{\rho_{\min}})$. Iterative schemes of quadratic coverage up to any positive integer order are developed for the solution of Kepler's equation. A sample of 110 systems is selected from the Sixth Catalog of Orbits (Hartkopf *et al.* 2001). Numerical studies are included and some important results are as follows: (1) there is no dependence between $\rho_{\max}$ and the spectral type and (2) a minor modification of Giannuzzi's (1989) formula for the upper limits of $\rho_{\max}$ functions of spectral type of the primary.

Key words. Stars: spectral types—binaries: visual—numerical: optimization.

1. Introduction

The maximum separations of the visual binaries are of interest in assessing the effects of chance encounters with neighboring stars and molecular clouds, and the effects of the general galactic potential. Also it is connected with the problem of binary formation. The dependence between maximum separations and spectral types of the components in visual binary systems have been studied by several authors (Öpik 1924; Halbwachs 1983, 1986; Abt 1986, 1988a, 1988b; Giannuzzi 1989). By using the published catalogs of known binaries, Öpik (1924) and Abt (1986) showed that there was an evolutionary decrease in binary separations with the spectral type of the primary. Moreover Öpik clearly showed that early-type visual binaries have greater angular separation on the average, at the same apparent magnitudes, than late-type binaries, even though the former were more distant. Therefore their separations in AU are much greater on the average. Abt (1986, 1988b) found a decrease of the

limiting upper separation from the early to late-type systems. Another study was done by Giannuzzi (1989) who showed that the result obtained by Abt was due to selective constraints.

Due to the importance of the maximum (minimum) separations among catalogued binaries, the present paper is devoted for two purposes. First, to establish a computational algorithm for maximum ($\rho_{\max}$) or minimum ($\rho_{\min}$) angular separations and the corresponding apparent position angles ($\theta|_{\rho_{\max}}, \theta|_{\rho_{\min}}$) for visual binary systems from their orbital elements. Second, to illustrate the applications of the algorithm for studying the upper limits of $\rho_{\max}$ as functions of spectral type.

2. Basic formulation

2.1 *Individual masses of a binary system*

The individual masses (M_a, M_b) of the components of binary systems, in solar units, could be computed (Reed 1984) from the knowledge of their apparent magnitudes (m_a, m_b), orbital period P (in years), and the semimajor axis a'' of the true orbit (in seconds of arc), by the equations

$$\log M_b = 15\left\{m_b + \alpha - \frac{5}{3}\log(1 + 10^{\Delta/\beta}) - \Gamma\right\} \Big/ \left(\frac{5}{3} + \beta\right), \tag{1}$$

$$M_a = M_b(10^{\Delta/\beta}), \tag{2}$$

where

$$\alpha = 4.5, \quad \beta = -9.5 \tag{3}$$

and

$$\Gamma = \frac{10}{3}\log P - 5\log \tilde{a} - 5. \tag{4}$$

2.2 *Two-body formulations*

The relative two-body problem is represented by the differential system

$$\ddot{\mathbf{r}} = -\frac{\mu}{r^3}\mathbf{r}, \tag{5}$$

where dots denote the second differentiation with respect to time t, and μ is the Gaussian constant. With the units usually used in double star computations, μ is given as

$$\mu = 4\pi^2(M_a + M_b)\,\pi''^3, \tag{6}$$

where π'' is the parallax. The relation between position and time t, for an elliptic orbit, is given by Kepler's equation as

$$\sqrt{\frac{\mu}{a^3}}(t - T) = E - e\sin E, \tag{7}$$

where T, e and E are respectively, the time of periastron passage, the eccentricity, and the eccentric anomaly.

The relation between the ephemerides (θ^0, ρ'') and r, f and the orientation angles are given as

$$\tan(\theta - \Omega) = \tan(f + \omega)\ \cos i, \tag{8}$$

$$\rho = r\ \cos(f + \omega)\ \sec(\theta - \Omega). \tag{9}$$

where θ is the apparent position angle and ρ is the angular separation. Equations (8) and (9) convert f and r of the true orbit into θ and ρ. Finally, the values of r and f in these equations are determined from

$$r = a\ (1 - e \cos E), \tag{10}$$

to avoid a possibility of numerical trouble when f is computed from the classical equation

$$f = 2 \tan^{-1} \left\{ \sqrt{\frac{1+e}{1-e}} \tan \frac{1}{2} E \right\},$$

for angles near 90°, we use the remarkably elegant formula (Broucke & Cefola 1972)

$$f = E + 2 \tan^{-1} \left\{ \frac{\sin E}{\nu - \cos E} \right\}, \tag{11}$$

where

$$\nu = \frac{1}{e} \left\{ 1 + \sqrt{1 - e^2} \right\}, \tag{12}$$

which is free of numerical trouble.

3. Computational developments

3.1 *Solution of Kepler's equation*

Kepler's equation (7) is usually solved by iteration methods. To apply any of these methods one needs (a) initial guess and (b) an iterative scheme. For the initial guess E_0, we use (Sharaf *et al.* 2000):

$$E_0 = M + \frac{e \sin M}{1 - \sin(M + e) + \sin M}, \tag{13}$$

where the mean anomaly M is given by

$$M = \left\{ \frac{\mu}{a^3} \right\}^{\frac{1}{2}} (t - T). \tag{14}$$

For the second point, that is, the iterative scheme, let us write equation (7) as

$$G(E) = E - e\sin E - M = 0. \tag{15}$$

Clearly G: $R \to R$ is a smooth map. Equation (15) has a solution $E = (\gamma)$ (say). To construct an iterative scheme for solving equation (15), some basic definitions are recalled as follows:

(1) The error in the nth iterate is defined as

$$\epsilon_n = \gamma - E. \tag{16}$$

(2) If the sequence (E_n) converges to $E = \gamma$,

$$\lim_{n\to\infty} E_n = \gamma. \tag{17}$$

(3) If there exists a real number p such that

$$\lim_{i\to\infty} \frac{|E_{i+1} - \gamma|}{|E_i - \gamma|^p} = \lim_{i\to\infty} \frac{|\epsilon_{i+1}|}{|\epsilon_i|^p} = K \neq 0, \tag{18}$$

we say that the iterative scheme is of order p at γ . The constant K is called the asymptotic error constant. For $p = 1$, the convergence is linear; for $p = 2$, the convergence is quadratic; for $p = 3, 4, 5$, the convergence is cubic, quartic and quintic respectively.

An iterative scheme for solving equation (15) includes derivatives of G as much as the order of the scheme. In fact, as it is clear from the above definitions, the higher the order of an iterative scheme, the higher its accuracy and rate of convergence will be.

Due to the simplicity of the derivative formulae of the trigonometric functions involved, we are encouraged to establish the solution of Kepler's equation, an iterative scheme of any desired order.

To achieve this scheme, Taylor series method (Broucke & Cefola 1972) is used by means of which, it is easy to form a class of iteration formulae, containing members of all integral orders to solve equation (15) as

$$E_{i+1} = E_i + \delta_{i,m+2};\ i = 0, 1, 2, \ldots;\ m = 0, 1, 2, \ldots, \tag{19}$$

$$\delta_{i,m+2} = \frac{-G_i}{\sum_{j=1}^{m+1} (\delta_{i,m+1})^{j-1} G_i^{(i)}/j!};\ \delta_{i,1} = 1;\ \forall i \geq 0, \tag{20}$$

$$G_i^{(j)} \equiv \frac{\mathrm{d}^j G(E)}{\mathrm{d}E^j}|_{E-E_i};\quad G_i \equiv G_i^{(0)}, \tag{21}$$

$$G_i{}^{(2r)} = (-1)^{r+1}\ e\ \sin\ E_i;\ r = 1, 2, \ldots, \tag{22}$$

$$G_i{}^{(2r+1)} = (-1)^{r+1}\ e\ \cos\ E_i;\ r = 1, 2, \ldots. \tag{23}$$

The convergence order is $m + 2$, and is given as

$$\epsilon_{i+1} = -\frac{1}{(m+2)!}\frac{G^{m+2}(\xi)}{G^{(1)}(\xi_1)}\epsilon_i^{m+2}, \tag{24}$$

where ξ is between E_{i+1}, E_i and ξ_1 is between E_{i+1} and γ.

3.2 *Minimization (maximization) process*

Since the tasks of maximization and minimization are trivially related to each other, we shall restrict the following analysis to the minimization process.

The objective function to be minimized is ρ given by equation (9) as

$$F \equiv \rho = r \cos s(f + \omega) \sec(\theta - \Omega),$$

where the corresponding apparent position angle θ is given by equation (8). Thus the problem of the minimum angular separation could be treated by any of the methods for one-dimensional unconstrained minimization. In these methods two algorithms are to be used. The first algorithm is to bracket the minimum from two given initial values of t as $\tilde{t}$ and $\tilde{t} + \Delta\tilde{t}$ (say). The second algorithm is to isolate the minimum by, for example, Golden Section Search or Brent's method. Full details of such algorithms could be found in Numerical Recipes Book (Press *et al.* 1992).

4. Numerical studies

FORTRAN 77 code was constructed for digital computations of the above formulations and applied to a sample of 110 systems selected from the Sixth Catalogue of Visual Binary Orbits such that $\Delta m \leq 0.2$. The results of the present section are presented in the following subsections.

4.1 *Calculations of* M_a, $(\rho_{\max}, \theta|_{\rho_{\max}})$ *and* $(\rho_{\min}, \theta|_{\rho_{\min}})$

The algorithm described above was used to calculate $(\rho_{\max}, \theta|_{\rho_{\max}})$ and $(\rho_{\min}, \theta|_{\rho_{\min}})$ for the binaries of the sample from their orbital elements. For minimizing the objective function (equation (9)) two subroutines were used, MNBRAK for bracketing the minimum and GOLDEN for isolating it. These subroutines are found in Press *et al.* (1992). The two initial values of the time $\tilde{t}, \tilde{t} + \Delta\tilde{t}$ needed for bracketing are taken as $\tilde{t} = T$ (in years) and $\Delta t =$ one year for all binaries of the sample. Finally, for the solution of Kepler's equation we used an iterative scheme of quantic convergence order ($p = 5$) with maximum number of iterations $N = 5$ and a stopping tolerance $= 10^{-10}$. The numerical results of this application are listed in Table 1. The designation of the table is: the first column is ADS number, the second column is apparent magnitude of the primary, the third column is the mass of the primary, the fourth column is minimum separation, the fifth column is the position angle at minimum separation, the sixth column is the maximum separation, and finally the position angle at maximum separation is listed in the seventh column.

Some statistical results could be obtained from these numerical results. Here we shall demonstrate one of them. The relation between the semi major axis ($\ddot{a}$) and the maximum separation ($\rho_{\max}$) for the selected binaries is plotted in Fig. 1. As it is clear, asymmetric distribution around the fitted line is well noticed. Fitting the data yield the linear relation

$$\log \ddot{a} = 1.0738 \log \ddot{\rho}_{\max} + 0.38 \tag{25}$$

with a correlation coefficient ($R = 0.82$), which indicate a relatively high correlation between the semi major axis and the maximum separation. Figure 2 presents

Table 1. Apparent magnitude (m_a) of the primary component, mass of the primary component (M_a), minimum ephemeredes ($\rho_{\min}$ and $\theta|_{\rho_{\min}}$) and maxium ephemeredes ($\rho_{\max}$ and $\theta|_{\rho_{\max}}$) of the 110 selected visual binaries.

ADS	m_a	M_a	$\rho_{\min}$	$\theta\|_{\rho_{\min}}$	$\rho_{\max}$	$\theta\|_{\rho_{\max}}$
....	6.40	1.99	0.38	14.52	157.4	7.7
15902	6.50	2.18	41.7	120.3	151.2	92.5
8891	8.10	1.85	8.29	74.67	314.3	134.3
14775	7.70	1.87	22.8	28.25	26.48	306.6
16314	3.00	2.04	30.0	34.46	112.4	206.8
7158	5.20	2.37	23.9	123.8	284.0	179.3
9744	4.30	3.96	0.22	0.743	348.1	157.8
4890	6.70	1.47	4.91	13.89	95.99	237.4
9505	6.10	1.75	6.54	10.44	319.3	140.2
2616	7.60	1.75	42.4	124.6	222.3	139.6
13944	6.60	2.69	15.4	133.3	268.7	148.6
3182	5.80	2.80	13.4	20.87	278.3	1.015
....	7.20	1.65	2.16	95.24	144.8	64.3
11842	5.70	1.69	20.5	57.11	37.60	30.0
....	6.90	1.74	37.3	47.52	266.8	86.17
....	7.80	1.97	55.7	83.57	260.1	82.47
14761	7.00	1.48	10.5	46.59	225.3	45.37
....	6.50	2.02	15.1	66.95	97.69	278.8
11574	8.50	1.38	1.85	21.58	186.3	96.41
8987	3.48	1.38	5.54	17.70	309.5	58.95
8987	7.80	1.38	11.0	37.48	1.699	221.3
8630	6.30	1.56	25.9	619.8	274.1	34.66
9689	6.30	1.60	20.7	88.37	58.87	237.4
....	7.50	1.35	9.17	24.29	274.7	183.8
4396	8.80	1.41	0.33	24.48	250.5	160.4
9247	6.00	1.42	16.0	26.92	78.38	264.6
3064	6.00	1.47	5.23	9.507	85.04	268.2
....	6.10	1.04	0.16	2.769	63.15	334.3
....	7.00	1.20	5.69	14.30	155.4	247.0
....	8.00	1.35	6.65	17.14	274.8	32.46
10421	6.40	1.45	12.1	31.08	70.65	152.3
15267	9.40	0.79	23.3	41.52	229.8	48.77
8804	7.50	1.00	18.5	43.77	82.03	196.2
9392	5.05	1.18	5.48	12.03	44.27	129.5
17052	7.60	1.21	23.9	176.2	279.2	32.30
3475	8.30	1.27	8.66	11.22	134.5	211.8
16539	8.10	1.28	1.98	8.961	78.01	347.5
10345	8.60	0.86	10.5	37.29	160.6	46.95
16800	5.20	1.07	5.54	13.57	163.3	69.78
....	7.00	1.20	4.10	10.04	231.2	51.21
14773	9.60	1.23	7.53	15.80	62.22	323.8
16819	5.65	1.26	5.84	9.630	136.0	45.73
11998	5.65	1.26	64.7	157.9	134.0	16.34
....	7.50	1.30	17.7	137.1	58.95	234.4
16819	7.20	1.31	9.71	42.41	119.4	226.9
6483	7.50	1.31	10.4	16.79	171.1	51.98
6811	8.10	1.36	3.04	7.712	303.7	32.57
10345	5.40	2.53	91.2	269.3	182.8	52.97
918	7.18	0.96	11.7	48.95	111.3	203.2
5871	8.30	1.25	2.26	15.63	312.0	221.3

Table 1. (*Continued*)

ADS	m_a	M_a	$\rho_{\min}$	$\theta\|_{\rho_{\min}}$	$\rho_{\max}$	$\theta\|_{\rho_{\max}}$
9557	8.00	1.28	27.2	903.0	108.0	297.1
3082	7.90	1.58	46.0	124.4	72.29	249.8
....	6.60	1.60	6.43	8.538	46.20	327.0
16138	7.60	0.89	18.8	35.17	52.02	318.9
1538	7.60	0.91	11.7	21.76	49.91	224.6
16138	8.20	0.92	31.4	117.0	77.94	299.4
6354	8.20	0.95	7.63	25.74	239.0	107.1
2236	7.80	0.98	9.82	76.06	63.58	321.2
1538	6.76	1.18	33.7	190.2	79.23	236.0
2236	6.76	1.18	5.88	20.90	76.86	178.4
9578	8.80	0.81	3.98	51.53	338.4	69.19
....	6.50	0.87	10.5	49.97	352.5	114.2
16644	9.40	0.88	3.42	15.48	341.7	254.6
17149	7.20	0.91	3.86	15.44	48.63	228.6
....	7.80	0.93	1.42	14.95	144.6	27.96
14893	7.33	0.98	27.9	55.45	234.4	339.4
5720	7.20	1.00	4.00	87.17	333.3	173.8
9182	7.50	1.02	36.6	182.5	232.2	351.3
2373	8.70	0.98	11.2	16.19	231.2	52.65
2524	8.30	1.16	17.8	48.42	154.5	321.7
7054	8.20	1.00	11.5	68.92	147.3	283.6
11483	6.80	1.24	57.8	165.6	191.5	23.80
13169	9.30	0.96	24.1	36.81	215.6	103.1
3701	5.70	0.60	8.22	19.24	128.1	298.1
2028	8.60	0.92	0.96	19.91	84.81	233.3
....	8.90	0.76	28.7	11043	272.1	136.2
363	8.90	0.76	14.1	69.41	15.37	220.0
363	7.20	0.82	3.69	20.96	71.04	164.6
520	9.00	0.72	8.61	14.26	66.80	295.7
8901	6.30	0.80	7.33	14.66	278.6	4.604
10871	8.60	0.86	12.8	34.78	75.71	255.2
2980	7.30	0.66	1.94	3.768	95.67	247.9
....	9.30	0.76	7.95	68.98	33.13	288.6
5949	8.20	1.20	18.7	28.11	148.0	328.0
....	2.90	2.95	19.49	332.6	51.27	263.4
....	6.00	1.63	2.424	4.402	157.6	297.2
7545	5.30	2.93	8.466	62.91	99.93	266.0
....	5.30	1.62	4.459	110.3	176.8	268.8
3391	7.30	2.14	12.62	27.87	231.4	95.35
6871	6.90	1.53	8.070	20.70	314.6	159.3
....	6.10	1.64	3.396	51.54	132.7	41.22
....	5.10	1.80	6.050	23.11	125.3	2.435
....	6.60	1.46	1.187	6.402	42.09	310.2
....	5.10	2.09	1.117	11.30	48.90	142.6
9159	8.30	1.65	39.04	105.8	98.59	287.6
16497	6.10	1.72	5.001	9.011	324.8	132.2
....	7.00	1.39	34.76	296.4	125.8	308.8
16497	6.10	1.73	47.30	83.68	225.2	96.41
....	5.60	1.58	12.84	71.57	4.641	271.0
....	5.60	1.21	3.473	15.37	33.29	125.1
....	7.00	1.66	13.29	97.66	355.4	141.2

Table 1. (*Continued*)

ADS	m_a	M_a	$\rho_{\min}$	$\theta\|_{\rho_{\min}}$	$\rho_{\max}$	$\theta\|_{\rho_{\max}}$
9909	4.90	1.49	3.218	16.21	228.5	318.6
999	8.00	1.15	1.331	6.680	198.9	110.6
....	6.90	1.15	23.47	305.3	53.85	201.8
11520	7.20	0.99	12.48	48.45	148.8	332.3
16098	9.00	0.86	4.967	47.32	271.0	92.21
3041	8.10	1.14	4.874	8.808	158.0	67.75
14783	7.00	1.15	7.844	10.35	331.3	226.9
....	7.20	1.19	5.575	38.03	305.8	199.6
10598	6.00	0.87	9.557	23.42	34.94	159.7

$\ddot{\rho}_{\max} - (\log \ddot{a}) - \ddot{\rho}_{\max}$) distribution with very low correlation coefficient ($R = 0.096$). This behavior is also obtained by many authors (e.g. Bartkevicius 2008).

4.2 *Upper limits of* $\rho_{\max}$

The second application is a preliminary study on the upper limits of $\rho_{\max}$ as functions of spectral types. Before starting, let us summarize the most important results of previous work on this subject.

4.2.1 *Summary of the previous work.* Abt (1988a, 1988b) showed that the reason for studying catalogued pairs is because they usually have data for long time intervals that show whether the members have common motions (no significant variation in separations and angles that cannot be attributed to orbital motion). Also it is found that maximum separations have upper limits as functions of spectral type of the primary components given by

$$d(AU) = 2500(M_a)^{1.54}. \tag{26}$$

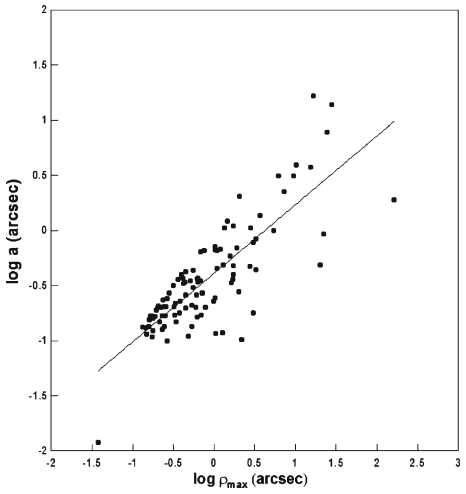

Figure 1. Relation of the semi-major axis and the maximum separation for selected binaries.

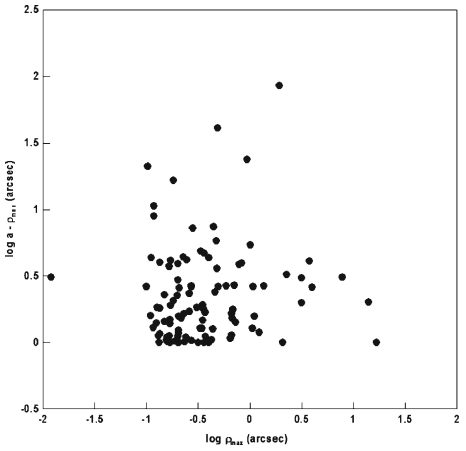

Figure 2. The correlation between the maximum separation ($\ddot{\rho}_{\max}$) and ($\log \ddot{a} - \ddot{\rho}_{\max}$).

It turns out that the main-sequence binaries have separations decreasing in the average from early to late types. The limit expressed by equation (26) is a catalogued limit, it is provided in order to avoid optical systems.

By examining visual binaries from the Yale Catalog of Bright Stars, Halbwachs (1983, 1986) found no significant variation in the statistics of the separations between the components where different spectral types of the primaries are concerned.

Giannuzzi (1989) used a sample of the solar neighboring visual binaries and enforced Halbwachs results and showed that the conclusion of Abt (1988a, 1988b) was probably due to selective constraints. Also, she suggested a formula for the upper limit as

$$d(AU) = 1.2\rho\ 10^{0.2m_a}(M_a)^{1.54}, \tag{27}$$

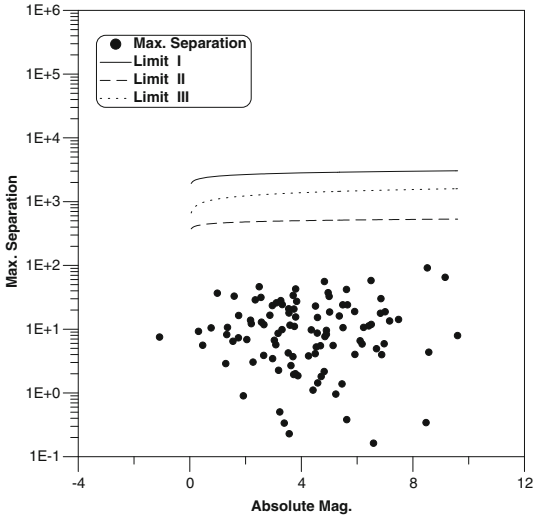

Figure 3. The three limits: limit I of equation (26), limit II of equation (27) and limit III of equation (28).

in which ρ is the first observed separation (due to the existence of the correlation between the semimajor axis and ρ, there is no matter to use ρ at any epoch).

4.2.2 *The present study.* From the previous subsection, two points are to be noted: First, Abt (1988b) selected the systems with common motion and take the tabulated largest value of the separation as the maximum value. Secondly, Giannuzzi (1989) referred to the separation in equation (27) as the first observed separation. On the other hand, Kuiper (1935) stated that it is not sufficient, however, to posses a set of binaries for which the separations at a standard epoch are known. Consequently, we use unique values for the separation which may be the maximum separation computed by the algorithm described in §3. The upper limit is thus given by

$$d(AU) = 1.2\rho_{\max}\ 10^{0.2m_a}(M_a)^{1.54}. \tag{28}$$

In Fig. 3 the maximum separation for each pair is plotted as a function of the combined absolute magnitude of the systems. The three curves represent the upper limits (limit I of equation (26), limit II of equation (27) and limit III of equation (28)) to the physical pairs. The frequency distribution of the maximum separation is plotted in Fig. 4 against log $\rho_{\max}$ and according to the spectral class of the primaries. It is clear that, there is no difference in the distribution of the maximum separation, which in turn means that there is no dependence between the maximum separation and the spectral types.

The frequency distribution of the three upper limits (Equations (26), (27), (28) respectively) against (d) and according to the spectral class of the primaries is plotted in Figures 5, 6 and 7. The same behavior can be noticed as the distribution of the maximum separation, i.e., there is no difference in the distribution for the different

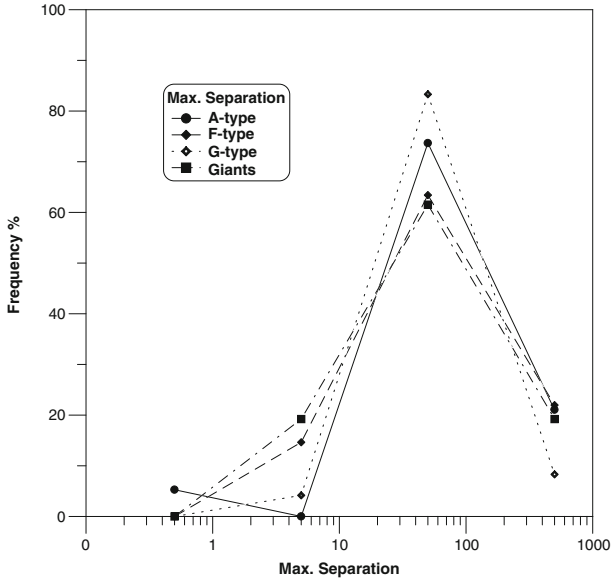

Figure 4. Frequency distribution of the maximum separation against log $\rho_{\max}$.

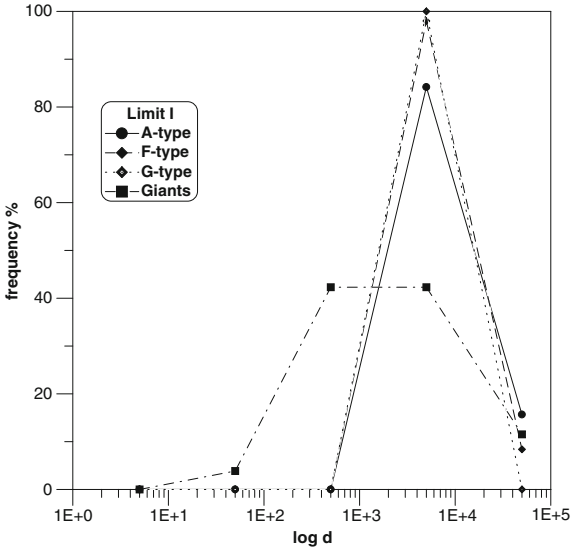

Figure 5. Frequency distribution of the upper limit of equation (26) against log d.

spectral types. The discrepancy appeared in Fig. 6 is probably due to the usage of the observed separation at a standard epoch in equation (26), which now disappeared when using the modified equation (28) as shown in Fig. 7.

In concluding the present paper, an efficient algorithm is established for computing $(\rho_{\max}, \theta|\rho_{\max})$, $(\rho_{\min}, \theta|_{\rho_{\min}})$ and the individual masses of visual binary systems.

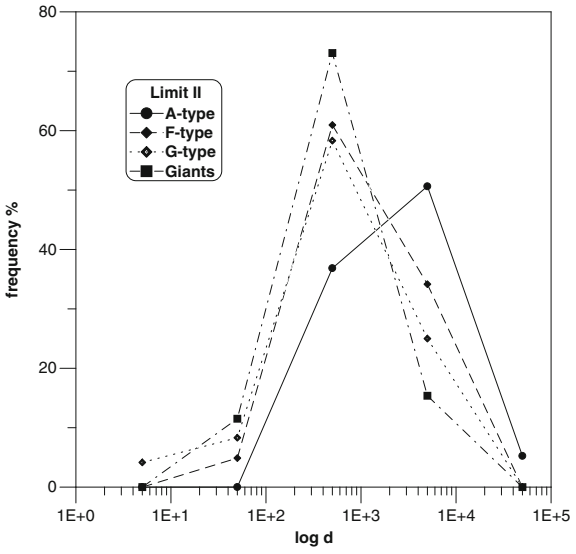

Figure 6. Frequency distribution of the upper limit of equation (27) against log d.

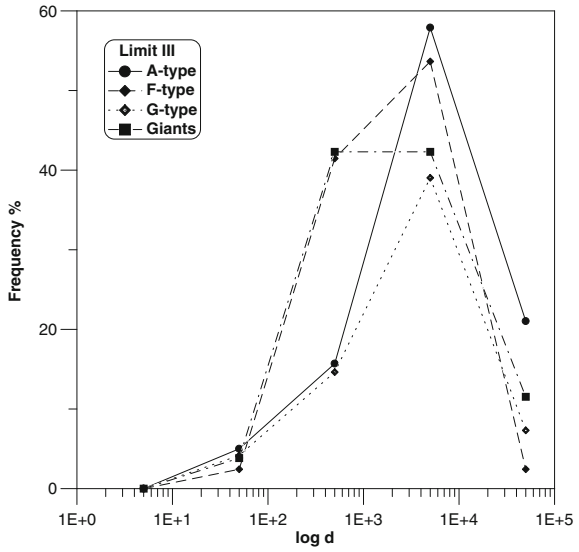

Figure 7. Frequency distribution of the upper limit of equation (28) against $\log d$.

The algorithm uses Reed's formula for the masses and a technique of one dimensional unconstraint minimization together with the solution of the Kepler's equation. Iterative schemes of quadratic up to any positive integer order are used for the solution of Kepler's equation. Some important results of numerical applications of the algorithm are: (1) there is no dependence between $\rho_{\max}$ and the spectral type, and (2) Giannuzzi's (1989) formula for the upper limits as functions of spectral type of the primary is modified as

$$d(AU) = 1.2\rho_{\max}\ 10^{0.2m_a}(M_a)^{1.54}.$$

References

Abt, H. A. 1986, *Astrophys. J.*, **304**, 688.
Abt, H. A. 1988a, *Astrophys. Space. Sci.* , **142**, 111.
Abt, H. A. 1988b, *Astrophys. J.*, **331**, 922.
Bartkevicius, A. 2008, *Baltic Astron.*, **17**, 209.
Broucke, R., Cefola, P. 1972, *Celestial Mech.*, **7**, 388.
Giannuzzi, M. A. 1989, *Astrophys. Space. Sci.*, **161**, 241.
Halbwachs, J. L. 1983, *Astron. Astrophys.*, **128**, 399.
Halbwachs, J. L. 1986, *Astron. Astrophys.*, **168**, 161.
Hartkopf, W. I., Mason, B. D., Worley, C. E. 2001, Sixth Catalog of Orbits of Vual Binary Stars, http://www.ad.usno.navy.mil/wds/orb6/orb6.html.
Kuiper, G. P. 1935, *Publ. Astron. Soc. Pacific.*, **47(15)**, 12.
Öpik, E. 1924, *Publ. Obs. Astro. Univ. Tartu.*, **25**, 6.
Press, W. H., Teukolsky, S. A., Vetterling, W. H., Flannery, B.P. 1992, Numerical Recipes (Cambridge Univ. Press).
Reed, B. C. 1984, *J. R. Astron. Soc. Can.*, **78(2)**, 83.
Sharaf, M. A., Abou-Elazm, M. S, Nouh, M. I. 2000, *Astr. Nach.* **1**, 321.